The 2009 IEEE/RSJ International Conference on
Intelligent Robots and Systems
October 11-15, 2009 St. Louis, USA

Dynamic Visual Servoing of a Small Scale Autonomous Helicopter in Uncalibrated Environments

Caizhi Fan, Baoquan Song, Xuanping Cai and Yunhui Liu, *Fellow,IEEE*

Abstract— **This paper presents a novel adaptive controller for image-based visual servoing of a small autonomous helicopter to cope with uncalibrated camera parameters and unknown 3-D geometry of the feature points. The controller is based on the backstepping technique but differs from the existing backstepping-based methods because the controller maps the image errors onto the actuator space via a depth-independent interaction matrix to avoid estimation the depth of the feature points. The new design method makes it possible to linearly parameterize the closed-loop dynamics by the unknown camera parameters and coordinates of the feature points in the three dimensional space so that an adaptive algorithm can be developed to estimate the unknown parameters and coordinates on-line. Two potential functions are introduced in the controller to guarantee convergence of the image errors and to avoid trivial solutions of the estimated parameters. The Lyapunov method is used to prove the asymptotic stability of the proposed controller based on the nonlinear dynamics of the helicopter. Simulations have been also conducted to demonstrate the performance of the proposed method.**

I. Introduction

THE small scale helicopter can perform various missions which cannot be performed by fixed-wing aircrafts because of its superior abilities in hovering, vertical takeoff and landing, and low-speed cruise. It has many potential applications in various areas including environment monitoring, anti-terrorism, and military operations. The academic challenges and great application perspectives have attracted extensive attention of researchers in recent years [1] [15]-[16].

Visual servoing has been one of the hottest topics in robotics for years. Two basic schemes: position-based visual servoing [9] and image-based visual servoing [10], have been developed for visually controlled robots. Image-based approaches employ directly the projections of feature points on the image plane as the feedback to the controller, and are considered simpler, more easily implemented and more robust to errors than position-based methods in which the position and orientation of the robot must be estimated. In image-based visual servoing, the underlying concept is the image Jacobian matrix which maps the image errors onto the joint space of the robot. The image Jacobian matrix depends on both the camera and the 3-D coordinates of the feature points. Calibrating the camera parameters at good accuracy is tedious, difficult and costly. It is usual that the 3-D coordinates of the feature points are not known to the robots. To cope with the uncertain camera parameters and the unknown 3-D coordinates, various adaptive controllers or on-line estimators of the image Jacobian matrix have been developed [6]- [8].

Compared to that of a robot manipulator, the dynamics of a helicopter is more complicated and difficult for its under-actuated property. When the visual servoing is addressed, the under-actuated and highly coupled dynamics further complicates the difficulties of the controller design. Only a few works can be found on visual servoing of helicopters. Most of existing controllers are subject to various assumptions. The visual servo controllers, developed in [1], assume that the optical axis of the camera coincides with the principal axis of the helicopter, which is hardly realized in real applications. The controllers proposed in [15][17] employed calibrated cameras. Zhang and Ostrowski [12] used the Lagrangian representation of the system dynamics to design an image-based controller for a blimp. In [13], Hamel and Mahony presented a novel image-based controller algorithm for under-actuated dynamic systems using the backstepping technique based on the passivity-like properties of the rigid body motion. They applied the controller to a helicopter [4] and an X4-flyer[16] and carried out experimental verifications. In our opinions, their work represents an important contribution to visual servoing of helicopters. However, the proposed method works with an accurately calibrated camera.

This paper copes with uncalibrated visual servoing of a small scale helicopter. We assume that the intrinsic and extrinsic parameters of the camera and the 3-D geometry of the feature points are unknown. As mentioned previously, the under-actuated dynamics complicates the design of a visual

This work is in part supported by National Natural Science Foundation of China under project 60675056 and the Hong Kong RGC under project 414707

Caizhi Fan, Baoquan Song, Xuanping Cai and Yunhui Liu are with the College of Electric Science and Engineering, National University of Defense Technology, ChangSha, China. caizhifan@gmail.com, baoquansong@gmail.com, xpcai@nudt.edu.cn, yhliu@mae.cuhk.edu.hk.

Yunhui Liu is also with the Department of Mechanical and Automation Engineering, The Chinese University of Hong Kong, Shatin, NT, Hong Kong.

servo controller for the helicopter. A new design method, which differs from what we developed for robot manipulators, has been proposed on the basis of the backstepping technique. Compared to existing backstepping-based methods, for example the method developed by Hamel and Mahony, in which the camera parameters are necessary, our controller uses a depth-independent interaction matrix to map the visual feedback to the actuator space to avoid estimation of the depth of the features. This new design method makes it possible to linearly parameterize the closed-loop dynamics using the unknown camera parameters and the unknown geometry. Therefore, we can use an adaptive algorithm, similar to that in[6][7], to estimate the parameters on-line using multiple images by minimizing the projection errors of the feature points on the image plane. Moreover, to avoid singularity of the depth-independent interaction matrix and obtaining trivial solutions in the parameter estimation, two potential functions are introduced in the controller. It is proved by Laypunov method that the proposed controller leads to convergence of the image errors to zero and that the estimated parameters are convergent to the real values up to a scale. Finally, simulations have been performed to demonstrate the performance of the proposed controller.

II. KINEMATICS AND DYNAMICS

A. Helicopter Dynamic Model

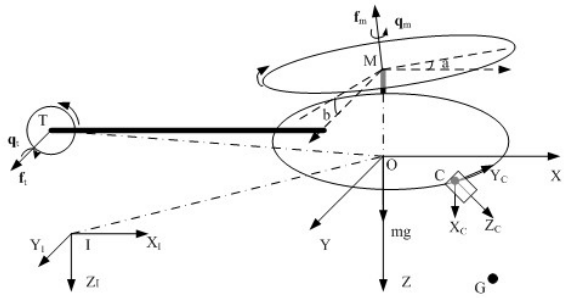

Fig. 1. An autonomous helicopter with a camera

Assume that the helicopter is a rigid body. Three coordinate frames as shown in Fig. 1, namely the inertial frame, the helicopter frame, and the camera frames, are set up to represent the positions and orientations of the helicopter and the camera. Let $\boldsymbol{\eta} = (\phi, \theta, \psi)^T$ denote the Euler angle. Let $\mathbf{R}$ be the rotation matrix of the helicopter with respect to the inertial frame. Let ${}^i\boldsymbol{\xi}(t)$ and ${}^i\mathbf{v}(t)$ denote the position and velocity of the helicopter with respect to the inertial frame, respectively. And let $\boldsymbol{\xi}(t)$ and $\mathbf{v}(t)$ denote the position and velocity represented in the helicopter frame, respectively. Let $\boldsymbol{\omega}(t)$ denote angular velocities of the helicopter with respect to the helicopter frame. Let m denote the mass and $\mathbf{I}$ represent the constant inertia tensor matrix around the mass center with respect to the helicopter frame. G is the feature point in the ground. In practice, the small body forces are ignored because they are much smaller than the magnitude of the force of the main rotor [2]-[5]. Thus, we will develop our work based on the following approximated dynamic model(the details can be seen in [3]):

$$ {}^i\dot{\boldsymbol{\xi}} = {}^i\mathbf{v} \tag{1}$$

$$ m\,{}^i\dot{\mathbf{v}} = -u\mathbf{R}\boldsymbol{\gamma}_3 + mg\boldsymbol{\gamma}_3 \tag{2}$$

$$ \dot{\mathbf{R}} = \mathbf{R}sk(\boldsymbol{\omega}) \tag{3}$$

$$ \mathbf{I}\dot{\boldsymbol{\omega}} = -\boldsymbol{\omega}\times\mathbf{I}\boldsymbol{\omega} - (c_1u + c_2)\boldsymbol{\gamma}_3 + \mathbf{P}\boldsymbol{\tau} \tag{4}$$

It has four inputs $(u, \boldsymbol{\tau}) = (u, \tau_x, \tau_y, \tau_z)$, the definition of $\mathbf{P}$ and $\boldsymbol{\tau}$ can be seen in [3].

B. Perspective Projection

Suppose that the camera is a perspective camera and the feature point is fixed on the ground and its coordinates are unknown.

Let ${}^i\mathbf{x}$ denote the coordinates of the position of the feature point in the inertial frame. The projection $\mathbf{y}(t)$ of the feature point on the image plane is given by

$$ \begin{bmatrix} \mathbf{y}(t) \\ 1 \end{bmatrix} = \frac{1}{{}^cz(t)}\mathbf{N}\mathbf{T}_h^{-1}(t)\begin{bmatrix} {}^i\mathbf{x} \\ 1 \end{bmatrix} \tag{5}$$

where $\mathbf{T}_h(t)$ is the homogenous transformation matrix of the helicopter with respect to the inertial frame and changes with motion of the helicopter. ${}^cz(t)$ denotes the depth of the feature point and $\mathbf{N}$ is the 3×4 perspective projection matrix depending on the intrinsic and extrinsic parameters. Let $\mathbf{n}_i^T$ denote the i-th row vector of the matrix $\mathbf{N}$.

By differentiating the eq. (5), we have

$$ \dot{\mathbf{y}}(t) = \frac{1}{{}^cz(t)}\times\underbrace{\left\{\begin{pmatrix}\mathbf{n}_1^T \\ \mathbf{n}_2^T\end{pmatrix} - \mathbf{y}(t)\mathbf{n}_3^T\right\}\begin{bmatrix}-\mathbf{E}_{3\times3} & sk(\mathbf{R}^T(t)\,{}^i\mathbf{x} - \boldsymbol{\xi}(t)) \\ \mathbf{0}_{1\times3} & \mathbf{0}_{1\times3}\end{bmatrix}}_{\mathbf{A}(\mathbf{R}(t),\boldsymbol{\xi}(t),\mathbf{y}(t))}\begin{bmatrix}\mathbf{v}(t) \\ \boldsymbol{\omega}(t)\end{bmatrix} \tag{6}$$

The matrix $\mathbf{A}(\mathbf{R}(t),\boldsymbol{\xi}(t),\mathbf{y}(t))$ is called as the depth-independent interaction matrix and its dimension is 2×6. The matrix $\mathbf{A}(\mathbf{R}(t),\boldsymbol{\xi}(t),\mathbf{y}(t))$ is determined by the camera parameters, the position and orientation of the helicopter, the projection and the unknown 3-D coordinates of the feature point. It is possible to use a parameter vector $\boldsymbol{\theta}_p$ to represent the products of the unknown camera parameters and the unknown 3-D coordinates of the feature point. The parameter vector $\boldsymbol{\theta}_p$ has 39 components. The perspective projection matrix which satisfies the eq. (5) is not unique. Therefore, we can fix one component of the unknown matrix

N. Here we fix the 3-rd row and 3-rd column component of the matrix **N** which is denoted by n_{33}. Without loss of generality, let n_{33}=1 so that we have the following 38 components to be estimated:

$$\boldsymbol{\theta}_p = (n_{kj}\,{}^i x_x, n_{kj}\,{}^i x_y, n_{kj}\,{}^i x_z, n_{11}, n_{12}, n_{13}, n_{14}, n_{21}, n_{22}, n_{23}, n_{24}, n_{31}, n_{32}, n_{34})^T \quad \forall k, j = 1,2,3 \tag{7}$$

where n_{kj} denotes the component in the k-th row and the j-th column of matrix **N** and ${}^i\mathbf{x} = ({}^i x_x, {}^i x_y, {}^i x_z)^T$. In the following sections we express an estimated value by using the variable with a cap "^".

III. Image-based Visual Servoing

A. Controller Design

This section presents an adaptive controller which uses the visual information to regulate the position of the helicopter. To simply the discussion we will consider the case when only one feature point is used. It is possible to extend the work to the case of multiple feature points. The objective here is to control the image errors to zero asymptotically. One feature point cannot constrain the position and attitude of the helicopter completely. Thus, we maintain the height and the yaw of helicopter simultaneously. The position and velocity of the helicopter can be measured by the DGPS. The Euler angle and the angular rate of the helicopter can be obtained from the IMU, and the visual information can be obtained by a camera mounted on the helicopter. The controller is designed by the backstepping technique. To linearly parameterize the closed-loop dynamics, we introduce the visual feedback at the last step of the backstepping procedure and use the depth-independent interaction matrix to map the image errors onto the actuator space of the helicopter.

Define the first error

$$\delta_1 = m\,{}^i\xi_z - m\,{}^i\overline{\xi}_z \tag{8}$$

where ${}^i\overline{\xi}_z$ denotes the desired height of the helicopter in the inertial frame. We further define the first energy function:

$$S_1 = \frac{1}{2}|\delta_1|^2 \tag{9}$$

Differentiating eq. (9) and considering the eq. (1) leads to

$$\dot{S}_1 = -\delta_1^2 + \delta_1(m\,{}^i v_z - m\,{}^i v_{dz}) \tag{10}$$

where ${}^i v_{dz}$ is the desired value for ${}^i v_z$ and we choose $m\,{}^i v_{dz} = -\delta_1$, and we want to hold the height of the helicopter so that ${}^i\dot{\overline{\xi}}_z = 0$.

Define $\delta_2' = m\,{}^i v_z - m\,{}^i v_{dz}$, then from (10) we have

$$\dot{S}_1 = -\delta_1^2 + \delta_1\delta_2' \tag{11}$$

We define the second error and energy function as follows:

$$\boldsymbol{\delta}_2 = (m\,{}^i v_x \quad m\,{}^i v_y \quad \delta_2')^T = m\,{}^i\mathbf{v} - m\,{}^i\overline{\mathbf{v}},\ S_2 = \|\delta_2\|^2/2 \tag{12}$$

where ${}^i\overline{\mathbf{v}} = (0 \quad 0 \quad {}^i v_{dz})^T$.

By differentiating S_2 and substituting eq. (2) into the derivative, we obtain

$$\dot{S}_2 = \boldsymbol{\delta}_2^T(-u\mathbf{R}(\boldsymbol{\eta})\boldsymbol{\gamma}_3 + mg\boldsymbol{\gamma}_3 - m\,{}^i\dot{\overline{\mathbf{v}}}) \tag{13}$$

Let $(\boldsymbol{\eta}_d, u_d)$ denote the desired values for $(\boldsymbol{\eta}, u)$ and define

$$\mathbf{X}_d = u_d\mathbf{R}(\boldsymbol{\eta}_d)\boldsymbol{\gamma}_3 \tag{14}$$

Let $\boldsymbol{\delta}_1' = (0,0,\delta_1)^T$, choose $\mathbf{X}_d = mg\boldsymbol{\gamma}_3 - m\,{}^i\dot{\overline{\mathbf{v}}} + \boldsymbol{\delta}_2 + \boldsymbol{\delta}_1'$.

Thus we have

$$\dot{S}_2 = -\|\boldsymbol{\delta}_2\|^2 - \boldsymbol{\delta}_2^T\boldsymbol{\delta}_1' + \boldsymbol{\delta}_2^T(\mathbf{X}_d - u\mathbf{R}(\boldsymbol{\eta})\boldsymbol{\gamma}_3) \tag{15}$$

In the third stage of the backstepping algorithm, we define the following two errors:

$$\boldsymbol{\delta}_3 = \mathbf{X}_d - u\mathbf{R}(\boldsymbol{\eta})\boldsymbol{\gamma}_3 \qquad \varepsilon_3 = \psi - \overline{\psi} \tag{16}$$

where $\overline{\psi}$ denotes the desired yaw angle of the helicopter and it is different from ψ_d generated by the backstepping algorithm via eq. (14). Consider the storage function

$$S_3 = \frac{1}{2}\|\boldsymbol{\delta}_3\|^2 + \frac{1}{2}|\varepsilon_3|^2 \tag{17}$$

Differentiating S_3 yields the following equation:

$$\dot{S}_3 = \boldsymbol{\delta}_3^T(\dot{\mathbf{X}}_d - (\dot{u}\mathbf{R}(\boldsymbol{\eta})\boldsymbol{\gamma}_3 + u\mathbf{R}(\boldsymbol{\eta})sk(\boldsymbol{\omega})\boldsymbol{\gamma}_3)) + \varepsilon_3(\dot{\psi} - \dot{\overline{\psi}}) \tag{18}$$

Here we extend the input u dynamically as follows[5]:

$$\ddot{u} = \tilde{u} \tag{19}$$

And the actual control u and its first derivative $\dot{u}$ become internal variables of the dynamic controller, $\tilde{u}$ is the nominal control input.

Consider the term associated with $\boldsymbol{\delta}_3$ of eq. (18) firstly. Let $(\boldsymbol{\omega}_d, \dot{u}_d)$ denote the desired values for $(\boldsymbol{\omega}, \dot{u})$. We define:

$$\begin{aligned}\mathbf{Y}_d &= \dot{u}_d\mathbf{R}(\boldsymbol{\eta})\boldsymbol{\gamma}_3 + u\mathbf{R}(\boldsymbol{\eta})sk(\boldsymbol{\omega}_d)\boldsymbol{\gamma}_3 \\ &= \dot{\mathbf{X}}_d + \boldsymbol{\delta}_2 + \boldsymbol{\delta}_3\end{aligned} \tag{20}$$

Eq. (20) can be rewritten as

$$\begin{bmatrix} 0 & u & 0 \\ -u & 0 & 0 \\ 0 & 0 & 1 \end{bmatrix}\begin{bmatrix} \omega_{dx} \\ \omega_{dy} \\ \dot{u}_d \end{bmatrix} = \mathbf{R}(\boldsymbol{\eta})^T(\dot{\mathbf{X}}_d + \boldsymbol{\delta}_2 + \boldsymbol{\delta}_3) \tag{21}$$

As seen in eq. (21), ω_{dz} does not appear and can be freely used to control the yaw. Consider the term associated with ε_3 of eq. (18). We choose the desired yaw as $\dot{\psi}_d = \dot{\overline{\psi}} - \varepsilon_3$.

The kinematical relationship between the Euler angles and the angular velocity of a rigid body is $\dot{\boldsymbol{\eta}} = \mathbf{W}_\eta^{-1}\boldsymbol{\omega}$ [5]. Replacing $\dot{\boldsymbol{\eta}}$ and $\boldsymbol{\omega}$ by $\dot{\boldsymbol{\eta}}_d$ and $\boldsymbol{\omega}_d$ respectively and assuming $\phi, \theta \in (-\pi/2, \pi/2)$, and considering $\dot{\psi}_d = \dot{\overline{\psi}} - \varepsilon_3$, we obtain

$$\omega_{dz} = (\cos\theta/\cos\phi)(\dot{\bar{\psi}} - \varepsilon_3 - (\sin\phi/\cos\theta)\omega_{dy}) \quad (22)$$

With the choices made above, eq. (18) is rewritten as

$$\begin{aligned}\dot{S}_3 &= -\|\boldsymbol{\delta}_3\|^2 - \boldsymbol{\delta}_3{}^T\boldsymbol{\delta}_2 - \varepsilon_3{}^2 + \varepsilon_3(\dot{\psi} - \dot{\psi}_d) \\ &+\boldsymbol{\delta}_3(\mathbf{Y}_d - (\dot{u}\mathbf{R}(\boldsymbol{\eta})\boldsymbol{\gamma}_3 + u\mathbf{R}(\boldsymbol{\eta})sk(\boldsymbol{\omega})\boldsymbol{\gamma}_3))\end{aligned} \quad (23)$$

At the last stage of the backstepping algorithm, we introduce the following error terms:

$$\boldsymbol{\delta}_4 = \mathbf{Y}_d - (\dot{u}\mathbf{R}(\boldsymbol{\eta})\boldsymbol{\gamma}_3 + u\mathbf{R}(\boldsymbol{\eta})sk(\boldsymbol{\omega})\boldsymbol{\gamma}_3) \quad \varepsilon_4 = \dot{\psi} - \dot{\psi}_d \quad (24)$$

The storage function associated with this stage of the backstepping is selected as

$$S_4 = \frac{1}{2}\|\boldsymbol{\delta}_4\|^2 + \frac{1}{2}|\varepsilon_4|^2 \quad (25)$$

Then, taking the derivative of S_4 yields

$$\begin{aligned}\dot{S}_4 &= \boldsymbol{\delta}_4{}^T(\dot{\mathbf{Y}}_d - (\ddot{u}\mathbf{R}(\boldsymbol{\eta})\boldsymbol{\gamma}_3 + 2\dot{u}\mathbf{R}(\boldsymbol{\eta})sk(\boldsymbol{\omega})\boldsymbol{\gamma}_3 \\ &+\mathbf{R}(\boldsymbol{\eta})sk(\boldsymbol{\omega})(sk(\boldsymbol{\omega})\boldsymbol{\gamma}_3) + u\mathbf{R}(\boldsymbol{\eta})sk(\dot{\boldsymbol{\omega}})\boldsymbol{\gamma}_3)) + \varepsilon_4(\ddot{\psi} - \ddot{\psi}_d)\end{aligned} \quad (26)$$

At this stage the control inputs enter into the equations through $\ddot{u} = \tilde{u}$, $\dot{\boldsymbol{\omega}}$ and $\ddot{\psi}$ as seen below.

To simplify the following analysis we define $\tilde{\boldsymbol{\tau}} = \dot{\boldsymbol{\omega}}$ and by transforming the eq. (4), we have

$$\tilde{\boldsymbol{\tau}} = -\mathbf{I}^{-1}\boldsymbol{\omega}\times\mathbf{I}\boldsymbol{\omega} - (c_1u + c_2)\mathbf{I}^{-1}\boldsymbol{\gamma}_3 + \mathbf{I}^{-1}\mathbf{P}\boldsymbol{\tau} \quad (27)$$

Thus, we have

$$\ddot{\psi} = -\boldsymbol{\gamma}_3{}^T\frac{d}{dt}(\mathbf{W}_\eta{}^{-1})\boldsymbol{\omega} + \sin\phi\sec\theta\tilde{\tau}_y + \cos\phi\sec\theta\tilde{\tau}_z \quad (28)$$

Then, the derivative of the last storage function in eq. (25) has the following form:

$$\begin{aligned}\dot{S}_4 &= \boldsymbol{\delta}_4{}^T[\dot{\mathbf{Y}}_d - 2\dot{u}\mathbf{R}(\boldsymbol{\eta})sk(\boldsymbol{\omega})\boldsymbol{\gamma}_3 - \mathbf{R}(\boldsymbol{\eta})sk(\boldsymbol{\omega})(sk(\boldsymbol{\omega})\boldsymbol{\gamma}_3) \\ &-(\tilde{u}\mathbf{R}(\boldsymbol{\eta})\boldsymbol{\gamma}_3 - u\mathbf{R}(\boldsymbol{\eta})sk(\boldsymbol{\gamma}_3)\tilde{\boldsymbol{\tau}})] + \varepsilon_4(\ddot{\psi} - \ddot{\psi}_d)\end{aligned} \quad (29)$$

Here, we will introduce the visual feedback in the controller. Denote the desired position of the feature point on the image plane by $\mathbf{y}_d$, which is a constant vector. The image error is obtained by measuring the difference between the current position and the desired one:

$$\Delta\mathbf{y}(t) = \mathbf{y}(t) - \mathbf{y}_d \quad (30)$$

where $\Delta\mathbf{y}(t)$ is the image error vector. To achieve the desired control, we choose

$$\begin{aligned}&\tilde{u}\mathbf{R}(\boldsymbol{\eta})\boldsymbol{\gamma}_3 - u\mathbf{R}(\boldsymbol{\eta})sk(\boldsymbol{\gamma}_3)\tilde{\boldsymbol{\tau}} \\ &= \dot{\mathbf{Y}}_d - 2\dot{u}\mathbf{R}(\boldsymbol{\eta})sk(\boldsymbol{\omega})\boldsymbol{\gamma}_3 - \mathbf{R}(\boldsymbol{\eta})sk(\boldsymbol{\omega})(sk(\boldsymbol{\omega})\boldsymbol{\gamma}_3) + \boldsymbol{\delta}_3 + \boldsymbol{\delta}_4 \\ &+\mathbf{R}(\boldsymbol{\eta})\hat{\mathbf{A}}_1{}^T(t)\mathbf{K}_1\Delta\mathbf{y}(t) + k_3\left\|\hat{\boldsymbol{\theta}}_p^T(t)\frac{\partial U_1(\hat{\boldsymbol{\theta}}_p(t))}{\partial\hat{\boldsymbol{\theta}}_p(t)}\right\|\boldsymbol{\delta}_4 + k_4\left\|\frac{\partial U_2(\hat{\boldsymbol{\theta}}_p(t))}{\partial\hat{\boldsymbol{\theta}}_p(t)}\right\|\boldsymbol{\delta}_4\end{aligned} \quad (31)$$

$$\begin{aligned}\ddot{\psi} &= \ddot{\psi}_d - \varepsilon_3 - \varepsilon_4 - \cos\phi\sec\theta\hat{\mathbf{A}}_2{}^T(t)\mathbf{K}_2\Delta\mathbf{y}(t) \\ &-k_3\left\|\hat{\boldsymbol{\theta}}_p^T(t)\frac{\partial U_1(\hat{\boldsymbol{\theta}}_p(t))}{\partial\hat{\boldsymbol{\theta}}_p(t)}\right\|\varepsilon_4 - k_4\left\|\frac{\partial U_2(\hat{\boldsymbol{\theta}}_p(t))}{\partial\hat{\boldsymbol{\theta}}_p(t)}\right\|\varepsilon_4\end{aligned} \quad (32)$$

The first five terms of eq. (31) and the first three terms of eq. (32) are obtained by the standard backstepping procedure. The terms $\mathbf{R}(\boldsymbol{\eta})\hat{\mathbf{A}}_1{}^T(t)\mathbf{K}_1\Delta\mathbf{y}(t)$ and $\cos\phi\sec\theta\hat{\mathbf{A}}_2{}^T(t)\mathbf{K}_2\Delta\mathbf{y}(t)$ represent the feedback of the image errors and can be represented as a linear form of the estimated parameters[6][7]:

$$\begin{aligned}\mathbf{R}(\boldsymbol{\eta})\hat{\mathbf{A}}_1{}^T(t)\mathbf{K}_1\Delta\mathbf{y}(t) &= \mathbf{R}(\boldsymbol{\eta})\mathbf{Y}_1(t)\hat{\boldsymbol{\theta}}_p(t) \\ \cos\phi\sec\theta\hat{\mathbf{A}}_2{}^T(t)\mathbf{K}_2\Delta\mathbf{y}(t) &= \cos\phi\sec\theta\mathbf{Y}_2(t)\hat{\boldsymbol{\theta}}_p(t)\end{aligned} \quad (33)$$

The last two terms of eqs. (31) and (32) are due to the potential functions used in the adaptive algorithm for on-line estimation of the parameters. $\mathbf{K}_1$ and $\mathbf{K}_2$ are 2×2 positive-definite gain matrices. k_3 and k_4 are scalar gains. $\hat{\mathbf{A}}_1{}^T(t)$ and $\hat{\mathbf{A}}_2{}^T(t)$ are parts of the estimated depth-independent interaction matrix and will be discussed in the subsection.

With the above choices, the derivative of S_4 has the form:

$$\begin{aligned}\dot{S}_4 &= -\|\boldsymbol{\delta}_4\|^2 - \boldsymbol{\delta}_4{}^T\boldsymbol{\delta}_3 - |\varepsilon_4|^2 - \varepsilon_4\varepsilon_3 \\ &-\boldsymbol{\delta}_4{}^T\mathbf{R}(\eta)\mathbf{Y}_1(t)\hat{\boldsymbol{\theta}}_p(t) - \varepsilon_4\cos\phi\sec\theta\mathbf{Y}_2(t)\hat{\boldsymbol{\theta}}_p(t) \\ &-(k_3\left\|\hat{\boldsymbol{\theta}}_p^T(t)\frac{\partial U_1(\hat{\boldsymbol{\theta}}_p(t))}{\partial\hat{\boldsymbol{\theta}}_p(t)}\right\| + k_4\left\|\frac{\partial U_2(\hat{\boldsymbol{\theta}}_p(t))}{\partial\hat{\boldsymbol{\theta}}_p(t)}\right\|)\|\boldsymbol{\delta}_4\|^2 \\ &-(k_3\left\|\hat{\boldsymbol{\theta}}_p^T(t)\frac{\partial U_1(\hat{\boldsymbol{\theta}}_p(t))}{\partial\hat{\boldsymbol{\theta}}_p(t)}\right\| + k_4\left\|\frac{\partial U_2(\hat{\boldsymbol{\theta}}_p(t))}{\partial\hat{\boldsymbol{\theta}}_p(t)}\right\|)|\varepsilon_4|^2\end{aligned} \quad (34)$$

From eq. (28), eq. (31) and eq. (32), the control input $(\tilde{u}, \tilde{\tau}_x, \tilde{\tau}_y, \tilde{\tau}_z)$ can be determined uniquely as long as $u \neq 0$. And then we can obtain the input u and the input $\boldsymbol{\tau}$ via eq. (19) and eq. (27), respectively.

B. On-line Parameters Estimation

To estimate the unknown parameters on-line, we use an algorithm similar to what developed in our previous work[6][7]. The idea is to minimize an error function that is linear to the parameters on-line using multiple images. Suppose that s images of the feature point have been captured at different time instants t_j $(j = 1, 2, ..., s)$ on the trajectory of the camera. For each image, we define the following error function:

$$\mathbf{e}_j(t) = {}^c\hat{z}(t,t_j)\mathbf{y}(t_j) - \hat{\mathbf{P}}(t)\mathbf{T}_h^{-1}(t_j)\begin{bmatrix}{}^i\hat{\mathbf{x}}(t)\\ 1\end{bmatrix} = \mathbf{W}(t_j)\hat{\boldsymbol{\theta}}_p(t) \quad (35)$$

where $\hat{\mathbf{P}}(t)$ is the matrix consisting of the first two rows of the matrix $\hat{\mathbf{N}}(t)$ .the matrix $\mathbf{W}(t_j)$ is a constant matrix for a fixed t_j and its value changes with change of t_j. The error $\mathbf{e}_j(t)$ varies with time. It is well known in computer vision that given a sufficient number s of images sequence, it is only possible to estimate the perspective projection matrix $\mathbf{N}$ and the coordinates of the feature point up to a scale[14]. Since there are 38 components in $\boldsymbol{\theta}$, 19 images are necessary for estimating the parameters. The proposed algorithm is to

estimate the unknown parameters by minimizing the error $\mathbf{e}_j(t)$. Obviously, the zero parameters vector is one of the solutions minimizing the error. To avoid the trivial solution, we introduce the following potential function:

$$U_1(\hat{\boldsymbol{\theta}}_p(t)) = 1/(e^{\alpha_1\|\hat{\boldsymbol{\theta}}_p(t)\|^2} - 1 + \beta_1) \tag{36}$$

where α_1 is a positive constant and β_1 is a small positive number.

Define $\mathbf{Y}_p^T(t) = \left[\mathbf{Y}_1^T(t)\mathbf{R}^T(\boldsymbol{\eta}) \quad \cos\phi\sec\theta\mathbf{Y}_2^T(t)\right] \quad \mathbf{o}(t) = [\boldsymbol{\delta}_4^T \quad \varepsilon_4^T]^T$

Then the adaptive rule is given by

$$\frac{d}{dt}\hat{\boldsymbol{\theta}}_p(t) = -\boldsymbol{\Lambda}^{-1}\left\{-\mathbf{Y}_p^T(t)\mathbf{o}(t) + \sum_{j=1}^{s}\mathbf{W}^T(t_j)\mathbf{K}_5\mathbf{e}_j(t) + \left(\frac{\partial U_1(\hat{\boldsymbol{\theta}}_p(t))}{\partial\hat{\boldsymbol{\theta}}_p(t)} + \frac{\partial U_2(\hat{\boldsymbol{\theta}}_p(t))}{\partial\hat{\boldsymbol{\theta}}_p(t)}\right)\|\mathbf{o}(t)\|^2\right\} \tag{37}$$

where $\boldsymbol{\Lambda}$ is a 38×38 positive-definite gain matrix. The first term on the right hand side of eq. (37)is to cancel the regression terms[11]. The second term represents on-line minimization of the errors $\mathbf{e}_j(t)$. $\mathbf{K}_5$ is a 2×2 positive-definite gain matrix. The first part of the last term is to pull the estimated parameters away from the zero values. The second part is due to another potential function which is introduced to guarantee the matrix $\hat{\mathbf{A}}_p(t)$ (see in next subsection) having a rank of 2.

C. Stability Analysis

For simplicity, we assume that the feature point is always visible during the motion so that its depth with respect to the camera frame is always positive.

Firstly, introducing the following non-negative function:

$$V(t) = S_1 + S_2 + S_3 + S_4 + \frac{1}{2}\hat{\boldsymbol{\theta}}_p^T(t)\boldsymbol{\Lambda}\hat{\boldsymbol{\theta}}_p(t) \tag{38}$$

By differentiating the non-negative function and considering (11), (15), (23), (34) and (37) together, we have

$$\begin{aligned}\dot{V}(t) &= \dot{S}_1 + \dot{S}_2 + \dot{S}_3 + \dot{S}_4 + \hat{\boldsymbol{\theta}}_p^T(t)\boldsymbol{\Lambda}\dot{\hat{\boldsymbol{\theta}}}_p(t)\\ &\le -|\delta_1|^2 - \|\boldsymbol{\delta}_2\|^2 - \|\boldsymbol{\delta}_3\|^2 - \|\boldsymbol{\delta}_4\|^2 - |\varepsilon_3|^2 - |\varepsilon_4|^2 - \sum_{i=1}^{s}\mathbf{e}_j^T(t)\mathbf{K}_5\mathbf{e}_j(t)\\ &\quad -\mathbf{o}^T(t)(k_3-1)\left\|\hat{\boldsymbol{\theta}}_p^T(t)\frac{\partial U_1(\hat{\boldsymbol{\theta}}_p(t))}{\partial\hat{\boldsymbol{\theta}}_p(t)}\right\|\mathbf{o}(t) - (k_4 - \|\hat{\boldsymbol{\theta}}^T(t)\|)\left\|\frac{\partial U_2(\hat{\boldsymbol{\theta}}(t))}{\partial\hat{\boldsymbol{\theta}}(t)}\right\|\|\mathbf{o}(t)\|^2\end{aligned} \tag{39}$$

We choose the gain k_3 is larger than 1, and choose the gain matrix $\boldsymbol{\Lambda}$ is a diagonal matrix. We select such the gain k_4 that $k_4 \ge \sqrt{2V(0)/\lambda_{\min}}$, where $\lambda_{\min}$ is the minimum component of the gain matrix $\boldsymbol{\Lambda}$.

From the above discussion, we can deduce that the function $V(t)$ never increases its value so that it is upper bounded. From the definition of $V(t)$, bounded $V(t)$ directly implies that the $\delta_1, \boldsymbol{\delta}_2, \boldsymbol{\delta}_3, \boldsymbol{\delta}_4, \varepsilon_3, \varepsilon_4, \mathbf{o}(t)$ and the estimated parameters are all bounded. In this paper we assume that the position coordinates of the helicopter in the inertial frame are bounded. Thus, from the definitions of $\delta_1, \boldsymbol{\delta}_2, \boldsymbol{\delta}_3, \boldsymbol{\delta}_4, \varepsilon_3, \varepsilon_4, \mathbf{o}(t)$ and the eq. (37) we can claim $\dot{V}(t)$ is uniformly continuous. From the Barbalat Lemma, we conclude that

$$\begin{aligned}&\lim_{t\to\infty}\delta_1 = 0, \lim_{t\to\infty}\boldsymbol{\delta}_2 = \mathbf{0}, \lim_{t\to\infty}\boldsymbol{\delta}_3 = \mathbf{0}, \lim_{t\to\infty}\boldsymbol{\delta}_4 = \mathbf{0}, \lim_{t\to\infty}\varepsilon_3 = 0,\\ &\lim_{t\to\infty}\varepsilon_4 = 0, \lim_{t\to\infty}\mathbf{o}(t) = \mathbf{0}, \lim_{t\to\infty}\mathbf{e}_j(t) = \mathbf{0}(j = 1,...,s)\end{aligned} \tag{40}$$

Consider the invariant set when $\dot{V}(t) = 0$, which must satisfy

$$\mathbf{R}(\boldsymbol{\eta})\hat{\mathbf{A}}_1^{\ T}(t)\mathbf{K}_1\Delta\mathbf{y}(t) = 0, \quad \cos\phi\sec\theta\hat{\mathbf{A}}_2^{\ T}(t)\mathbf{K}_2\Delta\mathbf{y}(t) = 0 \tag{41}$$

We can choose $\mathbf{K}_2 = \mu\mathbf{K}_1$ where μ is a positive scalar. Since the matrix $\mathbf{R}(\eta)$ has a rank of 3 and the term $\cos\phi\sec\theta$ is nonzero, the above equations are equivalent to the following equations:

$$\hat{\mathbf{A}}_p^T(t)\mathbf{K}_1\Delta\mathbf{y}(t) = [\hat{\mathbf{A}}_1\ (t) \quad \hat{\mathbf{A}}_2\ (t)]^T\mathbf{K}_1\Delta\mathbf{y}(t) = 0 \tag{42}$$

where $\hat{\mathbf{A}}_p(t)$ is a 2×4 matrix calculated by

$$\hat{\mathbf{A}}_p(t) = \left[\hat{\mathbf{A}}(t)(:,5) \quad -\hat{\mathbf{A}}(t)(:,4) \quad \hat{\mathbf{A}}(t)(:,3) \quad \hat{\mathbf{A}}(t)(:,6)\right]$$

where $\hat{\mathbf{A}}(t)(:,i)$ denotes the i-th column vector of the matrix $\hat{\mathbf{A}}(t)$. From LaSalle theorem, we can have the following result on the convergence:

$$\lim_{t\to\infty}\hat{\mathbf{A}}_p^T(t)\mathbf{K}_1\Delta\mathbf{y}(t) = 0 \tag{43}$$

The matrix $\hat{\mathbf{A}}_p(t)$ has a rank of 2 and the proof is omitted due to the constraint of space. Consequently, $\lim_{t\to\infty}\Delta\mathbf{y}(t) = 0$.

IV. Simulation

To evaluate the performance of the proposed visual servoing method, we have conducted a simulation on Hirobo Shuttle Plus(30 class engine). The physical and geometric parameters of the helicopter are based on estimations or rough measurement. m=4.5kg, $\mathbf{I}$=diag(0.17, 0.15, 0.1), l_1=0.232m, l_2=0.735m, l_3=0.0567m. The initial position, velocity and angular velocity of the helicopter are as follows:

$\boldsymbol{\xi}(0) = (13,-55,-55)^T m$, $\mathbf{v}(0) = (0,0,0)^T m/s$,$\boldsymbol{\omega}(0) = (0,0,0)^T rad/s$

The desired height, the desired yaw angle and the desired image position are $\overline{\xi}_z(t) = -55m$, $\overline{\psi}(t) = 0rad, \mathbf{y}_d = (382,280)^T pixels$.

The control gains are chosen as $\mathbf{K}_1$=2e-6diag(1,1), $\mathbf{K}_2$=2e-8diag(1,1), k_3=10, k_4=2e8, $\mathbf{K}_5$=1.5e-3diag(1,1), the constant coefficients are $\alpha_1 = 1, \beta_1 = 1e-4$. The real position of the feature point is ${}^i\mathbf{x} = (50,-50,-10)^T$. The real values of

the intrinsic parameters are $a_u = 871$ pixels, $a_v = 882$ pixels, $u_0 = 382$ pixels and $v_0 = 280$ pixels. The real extrinsic parameters matrix is:

$$\mathbf{T}_c = [-0.7071, 0, 0.7071, 0.4; 0, -1, 0, 0; 0.7071, 0.2; 0, 0, 0, 1]$$

The initial estimation of the unknown parameters are 30% difference from the true values.

Fig. 2a and Fig. 2b show the position and the Euler angle of the helicopter, respectively. Fig. 3a displays the position errors on the image plane. Fig. 3b shows one of the groups of the estimated projection errors. The simulation results confirmed the expected asymptotic convergence of the position errors on the image plane and the estimated projection errors to zero under the control of the proposed method.

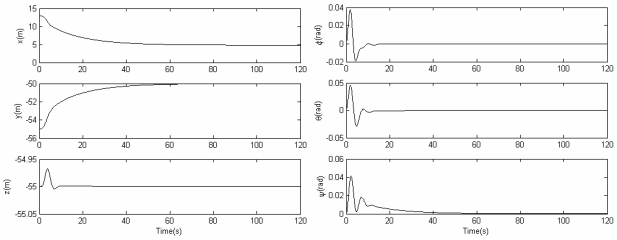

(a) (b)

Fig. 2 The position and Euler angle of the helicopter

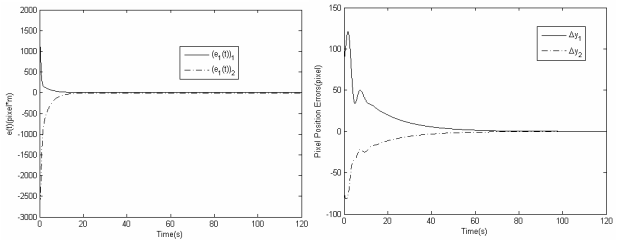

(a) (b)

Fig. 3 The profile of the estimated projection errors $\mathbf{e}_1(t)$ and the position errors on the image plane

V. CONCLUSION

This paper presented an image-based visual servoing method using the backstepping technique for a small scale autonomous helicopter when the camera is not calibrated and the 3-D coordinates of the feature points are unknown. The key concept lies in linear parameterization of the closed-based dynamics of the helicopter using the unknown parameters and coordinates. The linear parameterization is made possible by using the depth-independent interaction matrix to map the image errors onto the actuator space and incorporating the visual feedback into the controller design at the last step of the backstepping procedure. An adaptive algorithm is proposed to estimate the unknown parameters and coordinates based on on-line minimization of an error function. The Lyapunov method is used to prove the convergence of the position error on the image plane and the estimated projection error to zero. Finally, simulations were conducted to demonstrate the performance of the proposed method.

REFERENCES

[1] L. Mejias, P. Campoy, S. Saripalli and G. S. Sukhatme, "A visual servoing approach for tracking features in urban areas using an autonomous helicopter," in *Proc. of the 2006 IEEE Int. Conf. on Robotics and Automation*. Orlando, Florida, May 2006, pp. 2503-2508.

[2] J. T. Koo, S. Sastry, "Output tracking control design of a helicopter model based on approximate linearization", in *Proc. of the 37th Conference on Decision and Control*, Tampa, Florida, USA, 1998, pp. 3636-3640

[3] R. Mahony, T. Hamel and A. Dzul, "Hover control via Lyapunov control for an autonomous model helicopter," in *Proc. of the 38th Conf. on Decision & Control*, Phoenix, Arizona, USA, 1999, pp. 3490-3495.

[4] A. Chriette, T. Hamel and R. Mahony, "Visual servoing for a scale model autonomous helicopter," in *Proc. of the 2001 IEEE Int. Conf. on Robotics and Automation*, Seoul, Korea, 2001, pp. 1701-1706.

[5] R. Mahony and T. Hamel, "Robust trajectory tracking for a scale model autonomous helicopter," *International Journal of Robust and Nonlinear Control*, vol.14, pp. 1035-1059, 2004.

[6] H. Wang, Y. H. Liu and D. Zhou, "Dynamic visual tracking for manipulators using an uncalibrated fixed camera," *IEEE Trans. On Robotics*, vol. 23, no. 3, pp. 610-617, 2007

[7] Y. H. Liu, H. wang and K. Lam, "Dynamic visual servoing of robots in uncalibrated environments," in *Proc. of IEEE Int. Conf. on Robotics and Automation*, 2005, pp. 3142-3148.

[8] J. A. Piepmeier, G. V. McMurray and H. Lipkin, "Unclaibrated dynamic visual servoing," *IEEE Trans. on Robotics and Automation*, vol. 20, no.1, pp. 143-147, 2004.

[9] W. J. Wilson, C. C. W. Hulls, and G. S. Bell, "Relative end-effector control using Cartesian position based visual servoing," *IEEE Trans. on Robotics and Automation*, vol. 12, no. 5, pp. 684-696, 1996.

[10] B. Espiau, F. Chaumette, and P. Rives, "A new approach to visual servoing in Robotics," *IEEE Trans. on Robotics and Automation*, vol. 8, no. 3, pp. 313-326, 1992.

[11] J. J. Slotine and W. Li, "On the adaptive control of robot manipulators," *Int. J. Robotics Research*, Vol. 6, pp. 49-59, 1987.

[12] H. Zhang and J. P. Ostrowski, "Visual servoing with dynamics: Control of an unmanned blimp," in *Proc. IEEE Int. Conf. Robotics and Automation*, Detroit, MI, 1999, pp. 618-623.

[13] T. Hamel and R. Mahony, "Visual servoing of a class of under-actuated dynamic rigid-body systems," in *Proc. of the 39th Conf. on Decision and Control,* 2000, pp. 3933-3938.

[14] D. A. Forsyth and J. Ponce, Computer Vision: A Modern Approach. Englewood Cliffs, NJ: Prentice-Hall, 2003

[15] O. Shakerina, R. Vidal, C. S. Sharp, Y. Ma and S. S. Sastry, "Multiple-view motion estimation and control for landing and unmanned aerial vehicle," in *Proc. IEEE Int. Conf. Robotics and Automation*, May 2002, pp.2793-2798.

[16] N. Guenard, T. Hamel and R. Mahony, "A practical visual servo control for a unmanned aerial vehicle," in *IEEE International Conference on Robotics and Automation*, Roma, Italy, 2007, pp. 1342-1348.

[17] Kei Watanabe, Yuta Yoshihata, Yasuhi Iwatani and Koichi Hashimoto, "Image-based visual PID control of a micro helicopter using a stationary camera," in *SICE Annual Conference 2007*, Kagawa University, Japan, 2007, pp. 3001-3006.